Layer-wise Adaptive Step-Sizes for Stochastic First-Order Methods for Deep Learning

Achraf Bahamou
Department of Industrial Engineering
and Operations Research
Columbia University
New York, NY 10027

Donald Goldfarb
Department of Industrial Engineering
and Operations Research
Columbia University
New York, NY 10027

Abstract

We propose a new per-layer adaptive step-size procedure for stochastic first-order optimization methods for minimizing empirical loss functions in deep learning, eliminating the need for the user to tune the learning rate (LR). The proposed approach exploits the layer-wise stochastic curvature information contained in the diagonal blocks of the Hessian in deep neural networks (DNNs) to compute adaptive step-sizes (i.e., LRs) for each layer. The method has memory requirements that are comparable to those of first-order methods, while its per-iteration time complexity is only increased by an amount that is roughly equivalent to an additional gradient computation. Numerical experiments show that SGD with momentum and AdamW combined with the proposed per-layer step-sizes are able to choose effective LR schedules and outperform fine-tuned LR versions of these methods as well as popular first-order and second-order algorithms for training DNNs on Autoencoder, Convolutional Neural Network (CNN) and Graph Convolutional Network (GCN) models. Finally, it is proved that an idealized version of SGD with the layer-wise step sizes converges linearly when using full-batch gradients.

1 Introduction and Related Work

Stochastic gradient descent SGD [43], using either single or mini-batch samples, is widely used because it is parsimonious in terms of both iteration cost and memory usage, and generalizes well [20]. However, to be efficient and effective in practice, the learning rate needs to be chosen with great care. This is also the case for modified variants of SGD that incorporate momentum terms [41]; [35], which has been shown to speed up the convergence of SGD on smooth convex functions. In DNNs, other popular variants of SGD scale the individual components of the stochastic gradient using past gradient observations to reflect variations in the magnitude of the stochastic gradient components (especially between layers). Among these are ADAGRAD [8], RMSProp [49], ADADELTA [53], and ADAM [21], as well as the structured matrix scaling version SHAMPOO [16] of ADAGRAD, TNT [42] and MBF [2]. These methods are scale-invariant but still need to tune the base LR.

In deterministic settings, it is standard procedure to compute the step size to take along a descent direction to ensure that the objective function is reduced by a reasonable amount. This is done by computing the function value and gradient at possibly several trial points along the step direction until criteria, such as the Armijo-Wolfe conditions are satisfied. In a stochastic setting, not only is this inexact linesearch procedure very time consuming, it does not guarantee a decrease in the loss function if computations are based on mini-batches of data. Nonetheless, inexact line search methods have recently been extended to work with SGD [30, 51, 38].

Even more recently, adaptive learning rate methods, referred to as SPS (SGD with Polyak Stepsizes), have been proposed for stochastic optimization[28, 37, 26, 15, 44, 14]. These techniques utilize both

Preprint. Under review.

the loss values and gradient norms obtained from sampled points to automatically adjust the step size, and, under the *interpolation* condition, have been shown [13] to converge, linearly for functions that satisfy the Polyak-Lojasiewicz condition, and sublinearly at a rate of $O(\frac{1}{\sqrt{k}})$ for quasar (strongly) convex functions (i.e., those that are one-point convex with respect to the desired solution x^*.) However, their applicability is restricted by their need to have a good estimate of the optimal function value. Adaptive overall LRs based on stochastic versions of Barzilai-Borwein (BB) step-sizes have also been proposed for DNNs [27], using an approach that was first advanced in [48]. The method in [27] computes the DNN LR at the start of each epoch by estimating the curvature of the loss function using the inner product $s^\top y$, where y is the difference between exponentially decreasing moving averages of the stochastic gradients, computed at the end of the current and preceding epoch, and s is the full step taken in the current epoch, divided by the number of iterations in that epoch. Since $s^\top y$ can be negative, if $s^\top y < 0$, $|s^\top y|$ is used. Also, an adaptive LR approach based on estimating the local Lipschiz constant of the loss function as the ratio of the norm of the change in the stochastic gradient on a step to the norm of that step has been proposed and analyzed in [33].

In this paper, we propose a layer-wise adaptive learning rate method that lies between adaptive first-order methods and block diagonal approximate second-order methods. Specifically, we propose a method that uses a block-diagonal pre-conditioner matrix, where the block associated with each layer in the DNN is a scaled identity matrix with a judiciously chosen learning-rate, computed based on the local curvature information of the loss function. Crucially, our method has comparable memory requirements to those of first-order methods and avoids tuning the global learning-rate hyperparameter, while its per-iteration time complexity is increased by only roughly an additional mini-batch gradient computation and is much smaller than that of popular second-order methods (e.g. KFAC) for training DNNs. We note that our method is most closely related to, and in fact was motivated by, the *stochastic adaptive gradient descent method (SA-GD)* that was proposed in [56] for minimizing empirical loss functions that are self-concordant. We further note that SA-GD is not directly applicable to training DNNs, since the objective function that is minimized is not even a convex function of all of the network parameters.

2 Problem Formulation and Notation

The problem at hand involves minimizing functions of the form

$$F(\boldsymbol{W}) = \int \boldsymbol{f}(\boldsymbol{W}; x, y) dP(x, y) = \mathbb{E}[f(\boldsymbol{W}; \xi)],$$

where $\boldsymbol{W}$ is a vector in $\mathbb{R}^d$. This type of problem is commonly encountered in statistics and machine learning. However, computing the exact expectation is usually not feasible, as the distribution $P(x, y)$ is often unknown. Instead, one can use an estimate of the expectation by computing the sample mean over a set of training data, where each of the n data points is an input-output pair (x_i, y_i), which leads to the empirical risk minimization problem

$$F(\boldsymbol{W}) = \frac{1}{n} \sum_{i=1}^{n} \boldsymbol{f}\left(\boldsymbol{W}, (x_i, y_i)\right) = \frac{1}{n} \sum_{i=1}^{n} F_i(\boldsymbol{W}).$$

This can be done efficiently using stochastic optimization algorithms that randomly select mini-batches of data at each iteration,since using the full data set is often too large for classical optimization algorithms to handle.

In this paper, we consider a DNN with L layers, defined by weight matrices W_λ (including the bias), for each layer$\lambda \in [L]$, that transforms the input data $\boldsymbol{x}$ to the output $f(\boldsymbol{W}, \boldsymbol{x})$. For a data-point $(\boldsymbol{x}, y)$, the loss $\ell\left(f(\boldsymbol{W}, \boldsymbol{x}), y\right)$ between the output $f(\boldsymbol{W}, \boldsymbol{x})$ and the label y, is a non-convex function of $\boldsymbol{W} = \left[\mathrm{vec}\left(W^{(1)}\right)^\top, ..., \mathrm{vec}\left(W^{(L)}\right)^\top\right]^\top \in \mathbb{R}^d$, containing all of the network's parameters, concatenated together, (vec(A) denotes the vectorization of a matrix A by stacking its columns), and ℓ measures the accuracy of the prediction (e.g. squared error loss, cross-entropy loss). The optimal parameters are obtained by minimizing the average loss F over the training set:

$$F(\boldsymbol{W}) = \frac{1}{n} \sum_{i=1}^{n} \ell(f(\boldsymbol{W}, \boldsymbol{x}_i), y_i), \tag{1}$$

This setting is applicable to most common models in deep learning such as Multilayer Perceptrons (MLPs), Convolutional Neural Networks (CNNs), Graph Convolutional Networks (GCNs), etc. In these models, the trainable parameters $W^{(\lambda)}$ ($\lambda = 1, \ldots, L$) come from the weights and bias of each layer, whether it be a feed-forward, convolutional, recurrent, etc.

We consider iterative methods that take the following form: at the k-th iteration, we draw m i.i.d samples $S_k = \{\xi_{i_1}, \ldots, \xi_{i_m}\} = \{(\boldsymbol{x}_{i_1}, y_{i_1}), \ldots, (\boldsymbol{x}_{i_m}, y_{i_m})\}$ and define the sub-sampled objective function and its sub-sampled gradient and Hessian at the current weight vector $\boldsymbol{W}_k$ as

$$F_{S_k}(\boldsymbol{W}_k) = \frac{1}{m}\sum_{i\in S_k} \ell(f(\boldsymbol{W}_k, \boldsymbol{x}_i), y_i) = \frac{1}{m}\sum_{i\in S_k} F_i(\boldsymbol{W}_k),$$
$$g_k = \nabla F_{S_k}(\boldsymbol{W}_k) = \frac{1}{m}\sum_{i\in S_k} \nabla F_i(\boldsymbol{W}_k), \quad H_k = \nabla^2 F_{S_k}(\boldsymbol{W}_k) = \frac{1}{m}\sum_{i\in S_k} \nabla^2 F_i(\boldsymbol{W}_k).$$

We are clearly assuming here, that F_{S_k} is twice-differentiable at all points encountered by our methods, even if our model uses activation functions such as ReLU, that are not even differentiable everywhere. See the remarks regarding the Hessian recurrence (5) below. An iteration of a first-order method based on these approximations is then given by

$$\boldsymbol{W}_{k+1} = \boldsymbol{W}_k - t_k d_k, \tag{2}$$

where t_k is a global step size, d_k is the descent direction, and S_k is the set of samples that is used to estimate the gradient and Hessian. For layer λ, we denote by $F_{S_k}^{(\lambda)}$ the restricted loss function that maps the weights $W_k^{(\lambda)}$ to $F_{S_k}(\boldsymbol{W}_k)$ with the other weight matrices $W_k^{(j)}, j \neq \lambda$ fixed, where $\boldsymbol{W}_k = \left[W_k^{(1)}, ..., W_k^{(L)}\right]^\top$. Similarly, we define the sub-sampled layer-wise gradient and Hessian as

$$g_k^{(\lambda)} = \nabla F_{S_k}^{(\lambda)}\left(W_k^{(\lambda)}\right) = \frac{1}{m}\sum_{i\in S_k} \nabla_{W_k^{(\lambda)}} F_i(\boldsymbol{W}_k), \quad H_k^{(\lambda)} = \nabla^2 F_{S_k}^{(\lambda)}\left(W_k^{(\lambda)}\right) = \frac{1}{m}\sum_{i\in S_k} \nabla^2_{W_k^{(\lambda)}} F_i(\boldsymbol{W}_k).$$

Denoting the layer-wise step-size for layer λ by $t_k^{(\lambda)}$, an iteration of a layer-wise version of (2) is given by:

$$W_{k+1}^{(\lambda)} = W_k^{(\lambda)} - t_k^{(\lambda)} d_k^{(\lambda)}, \quad \text{for } \lambda = 1\ldots., L. \tag{3}$$

3 Basis for Layer-wise Adaptive Learning Rate Method

Our proposed method is based on several known results. First, as first shown by Nesterov and Nemirovski [34], there is a formula for computing step-sizes that guarantees an improvement in the objective function when applying iterative descent methods to minimize a self-concordant function. Second, as shown in [55] and [1], several comonly used loss functions are self-concordant. Third, as shown in [4], for feed-forward DNNs that employ certain activation functions such as ReLU, if the loss function is a convex function of the outputs of the DNN, then the diagonal Hessian blocks associated with each layer are positive semi-definite. Moreover, it is then clear that if weight decay or quadratic regularization is incorporated into such a DNN model, these diagonal blocks of the Hessian will be positive definite. Furthermore, one can show, using results in [47], that the associated restricted loss function $F_{S_k}^{(\lambda)}$ is standard self-concordant, if we assume that the loss function is general self-concordant [1], which is less restrictive than standard self-concordance. By combining these results, we are able to develop a layer-wise closed-form step-size procedure for training DNNs.

Step-Sizes for Self-concordant Functions: Self-concordant functions were introduced by Nesterov and Nemirovski in the context of interior-point methods [34], and are defined as follows:

Definition 1. *A convex function $f : \mathbb{R}^n \to \mathbb{R}$ is self-concordant if there exists a constant c such that for every $x \in \mathbb{R}^n$ and every $h \in \mathbb{R}^n$, we have :*

$$\left|\nabla^3 f(x)[h,h,h]\right| \leq c\left(\nabla^2 f(x)[h,h]\right)^{3/2},$$

f is standard self-concordant if the above is satisfied for $c = 2$.

Many problems in machine learning have self-concordant formulations: In [55] and [1], it is shown that regularized regression, with either logistic loss or hinge loss, is self-concordant and variants

of Newton's method applied to these functions are analyzed. In deterministic setting (i.e $m = n$), methods that use the iterative scheme specified in (2) to minimize a self-concordant function and compute an adaptive step size

$$t_k^* = \frac{\rho_k}{(\rho_k + \delta_k)\,\delta_k}; \quad \text{where } \rho_k = g_k^T d_k, \text{ and } \delta_k = \|d_k\|_{\boldsymbol{W}_k} = \sqrt{d_k^T H_k d_k},$$

have been analyzed in [50] and [9]. In the latter paper, the above choice of t_k is shown to guarantee a decrease in the function value. Specifically, it is proved that

Lemma 1. *(Lemma 4.1, [9]) For F standard self-concordant, for all $0 \leq t < \frac{1}{\delta_k}$:*

$$F(x_k - t d_k) \leq F(x_k) - \Delta(\delta_k, t), \tag{4}$$

where $\Delta(\delta_k, t) = (\delta_k + \rho_k)t + log(1 - \delta_k t)$.

If $t = t_k^*$ then $F\left(x_k - t_k d_k\right) \leq F\left(x_k\right) - \omega\left(\eta_k\right)$, where $\eta_k = \frac{\rho_k}{\delta_k}$ and $\omega(z) = z - \log(1 + z)$. The latter results allow one to prove the linear convergence of such iterative methods by controlling the bound on the improvement of the loss function in every iteration.

Hessian structure in Feed-forward Neural Networks: Consider a feed-forward neural network that takes the single sample input $a^{(0)} = x$ and produces the output vector $h^{(L)}$ on the final layer L of the network, during the forward pass computation:

$$h^{(\lambda)} = W^{(\lambda)} a^{(\lambda-1)}; \quad a^{(\lambda)} = f_\lambda\left(h^{(\lambda)}\right) \quad 1 \leq \lambda < L,$$

where in layer λ, $h^{(\lambda)}$ and $a^{(\lambda)}$ are, respectively, vectors of pre- and post- activation values, and f_λ is the element-wise activation function. The pre-activation Hessian for layer λ is defined as $\left[\mathcal{H}^{(\lambda)}\right]_{i,j} = \frac{\partial^2 F}{\partial h_i^{(\lambda)} \partial h_{\lambda,j}^{(\lambda)}}$. One can show that the sub-sampled Hessian of $W^{(\lambda)}$ can be expressed as:

$$H^{(\lambda)} = \frac{\partial^2 F}{\partial \operatorname{vec}\left(W^{(\lambda)}\right) \partial \operatorname{vec}\left(W^{(\lambda)}\right)} = \left(a^{(\lambda-1)} a^{(\lambda-1)\top}\right) \otimes \mathcal{H}^{(\lambda)}.$$

In [4], it is shown that the pre-activation Hessian $\mathcal{H}^{(\lambda)}$ can be computed recursively as:

$$\mathcal{H}^{(\lambda)} = B^{(\lambda)} W^{(\lambda+1)\top} \mathcal{H}^{(\lambda+1)} W^{(\lambda+1)} B^{(\lambda)} + D^{(\lambda)}, \quad 1 \leq \lambda < L, \tag{5}$$

where $B^{(\lambda)} = \operatorname{diag}\left(f_\lambda'\left(h^{(\lambda)}\right)\right)$ and $D^{(\lambda)} = \operatorname{diag}\left(f_\lambda''\left(h^{(\lambda)}\right) \frac{\partial F}{\partial a^{(\lambda)}}\right)$ are diagonal matrices, and f_λ' and f_λ'' are the first and second derivatives of f_λ. The recursion is initialized with $\mathcal{H}^{(L)}$, which depends on the objective function and is easily calculated analytically for typical loss functions; for example for squared loss, $\mathcal{H}^{(L)} = I$. For a minibatch of samples S, the recursion is applied to each datapoint and the parameter Hessian is computed as the average of the individual sample Hessians.

In recent years piece-wise linear activation functions, such as the ReLU function $f(x) = \max(x, 0)$, have become popular. It has been argued that in contrast to the standard sigmoidal functions, they don't saturate which prevents the problem of exploding/vanishing gradients. Since the second derivative f'' of a piece-wise linear function is zero everywhere, the matrices $D^{(\lambda)}$ in the recursion will be zero (away from non-differentiable points). It follows that if $\mathcal{H}^{(\lambda)}$ is positive semi-definite (psd), which is the case for the most commonly used loss functions, **the block diagonal Hessian matrices are psd for every layer**. Additionally, if we add an L2 regularization term to the loss function, the restricted loss $F_{S_k}^{(\lambda)}$ function for each layer λ is **strictly convex**. Using results in [47], if one assumes that the loss function is general self-concordant, then the restricted loss $F_{S_k}^{(\lambda)}$ becomes standard self-concordant. Consequently, we can exploit Lemma 1 to develop closed-form layer-wise step-sizes and combine them judiciously to obtain a loss decrease. We note that one can only guarantee that the mini-batch loss is decreased if one employs a block-coordinate descent strategy.

We numerically investigated the Hessian blocks as well as the full Hessian spectrum of a trained simple 3-layer GCN with the following node-sizes $[1433, 128, 64, 7]$, on the Cora data set using vanilla Adam for 20 epochs. We exploited the scalable framework proposed in [11] that enables fast computation of the full and block Hessian eigenvalue/spectral density, using the Stochastic Lanczos

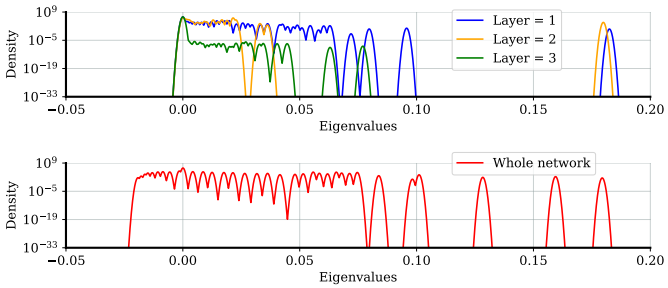

Figure 1: Hessian eigenvalues density estimations using Stochastic Lanczos Quadrature method.

Quadrature method, and report the results in Figure 1. We observe that the eigenvalues of the diagonal blocks of the Hessian corresponding to the 3 layers are all positive, whereas the full Hessian has a non-trivial set of small negative eigenvalues. We also notice that the union of the supports of the diagonal block-Hessian eigenvalues substantially overlaps the positive support of the full Hessian, indicating that the block diagonal approximation to the Hessian is not unreasonable.

A layer-wise step-sizes procedure: Based on the above arguments, we propose Algorithm 1 that gives the pseudo-code for a generic version of the layer-wise procedure for any optimization algorithm that produces a direction d_k at iteration k.

Algorithm 1: X-LW: Algorithm X with Layer-Wise Step-Sizes

Input: Initial $\boldsymbol{W}_0$, batch size m, number of iterations N and Algorithm X hyper-parameters.
for $k = 1 \cdots N$ **do**
  Sample m samples S_k.
  Compute $g_k = \nabla F_{S_k}(\boldsymbol{W}_k)$.
  Compute d_k Algorithm X direction.
  for $\lambda = 1 \dots L$ **do**
    Compute $\rho^{(\lambda)} = {d_k^{(\lambda)}}^\top g_k^{(\lambda)}$, $\delta^{(\lambda)} = \sqrt{{d_k^{(\lambda)}}^\top H_k^{(\lambda)} d_k^{(\lambda)}}$
    Compute $t_k^{(\lambda)} = \frac{1}{L} \frac{\rho^{(\lambda)}}{\left(\rho^{(\lambda)} + \delta^{(\lambda)}\right)\delta^{(\lambda)}}$
    $W_{k+1}^{(\lambda)} \leftarrow W_k^{(\lambda)} - t_k^{(\lambda)} d_k^{(\lambda)}$

In Section 6 below, we propose a practical version of the algorithm for both SGD with momentum and AdamW. However, we first present theoretical results for the linear convergence of the version of Algorithm 1 applied to vanilla SGD in the full batch setting.

4 Linear Convergence

In this section, we provide a linear convergence guarantee for vanilla gradient descent with Layer-Wise Step-Sizes, Procedure(SGD-LW), with exact gradients (i.e. the deterministic case with full batch $m = n$). Our theoretical analysis is based on the following technical assumptions on F:

A1. **Hessian regularity:** There exist $M \geq m > 0$ s.t $\forall \boldsymbol{W} \in \mathbb{R}^n$, $mI \preceq \nabla^2 F(\boldsymbol{W}) \preceq MI$.

A2. **B–Bounded iterates and Gradient regularity:** There exists $B > B_0 > 0$ with $\boldsymbol{W}^* \in \mathbb{B}$, $\mathbb{B} \equiv$the ball of radius B centered at 0, such that if $\boldsymbol{W}_0$ is chosen in $\mathbb{B}$, then the sequence of iterates $\{\boldsymbol{W}_k\}_{k=0}^{\infty}$ produced by the algorithm is contained within $\mathbb{B}$. Furthermore, we assume that F has bounded gradients within $\mathbb{B} : \exists\ \gamma > 0,\ \forall\ \boldsymbol{W} \in \mathbb{B}$: $\|\nabla F(\boldsymbol{W})\|_2 \leq \gamma$.

A3. **Layer-wise self-concordance:** F is layer-wise standard self-concordant, i.e for each layer $\lambda = 1 \cdots L$, the restricted function $F^{(\lambda)}$ is standard self-concordant.

The bounded gradient assumption A2 can be viewed as a technical assumption to simplify the proofs, as gradients of many common self-concordant functions can be unbounded. This assumption is equivalent to assuming that the algorithm is not divergent and the iterates stay within a bounded

region in which we can assume that the gradient is bounded **locally**. Note that there are no functions F that are strongly convex and for which the gradients are **globally** bounded.

Recent work [36] [24] [10] has shown that SGD can be proved to converge without requiring A2. Extending these ideas to our setting is a subject for further research. By using Lemma 1 in a judicious manner, we can control the loss improvement in every iteration to obtain linear convergence of the Algorithm SGD-LW:

Theorem 1. *Suppose that F satisfies Assumptions A1-A3. Let $\boldsymbol{W}_k$ be the iterates generated by taking the layer-wise steps $t_k^{(\lambda)}$ at iteration k for the Algorithm SGD-LW with full batch (i. e $m = n$), starting from any $\boldsymbol{W}_0$. Then, for any k, we have :*

$$(F(\boldsymbol{W}_k) - F(\boldsymbol{W}^*)) \leq \rho^k (F(\boldsymbol{W}_0) - F(\boldsymbol{W}^*)), \text{ where } \rho = 1 - \frac{m}{ML(1 + \frac{\gamma}{\sqrt{m}})}.$$

See Appendix A.2 for a proof of Theorem 1.

5 Implementation Details and Practical Considerations

Hessian vector product and computational complexity: In our framework, we need to compute the curvature along mini-batch stochastic gradient based directions $d_k^{(\lambda)}$, given by their **local norms**: $\delta^{(\lambda)} = \sqrt{{d_k^{(\lambda)}}^\top H_k^{(\lambda)} d_k^{(\lambda)}}$, for all layers λ. Hence we need to efficiently compute the Hessian-vector products $H_k^{(\lambda)} d_k^{(\lambda)}$. Fortunately, for functions that can be computed using a computational graph (Logistic regression, DNNs, etc) there are automatic methods available for computing Hessian-vector products exactly [40], which take about as much computation as gradient evaluations. **Hence, $H_k^{(\lambda)} d_k^{(\lambda)}$ can be computed with essentially the same effort as that needed to compute $g_k^{(\lambda)}$.** The method described in [40] is based on the differential operator:

$$\mathcal{R}\{F(\boldsymbol{W})\} = (\partial/\partial r) F(\boldsymbol{W} + r\boldsymbol{d})|_{r=0}\,.$$

Since $\mathcal{R}\{\nabla_{\boldsymbol{W}} F\} = Hd$ and $\mathcal{R}\{\boldsymbol{W}\} = d$, to compute Hd, [40] applies $\mathcal{R}$ to the back-propagation equations used to compute ∇F.

Exponentially moving averages, amortized updates and weight-decay: We use moving averages to both reduce the stochasticity and incorporate more information from the past; more specifically, we use a moving average scheme to get a better estimate of the layer-wise learning rates, i.e.$t_{k+1}^{(\lambda)} = \beta_t t_k^{(\lambda)} + (1-\beta_t)\frac{\rho^{(\lambda)}}{L\left(\rho^{(\lambda)}+\delta^{(\lambda)}\right)\delta^{(\lambda)}}$ with $\beta_t = 0.99$. The extra work for the $\frac{\rho^{(\lambda)}}{\left(\rho^{(\lambda)}+\delta^{(\lambda)}\right)\delta^{(\lambda)}}$ computation compared with first-order methods is amortized by only performing the updates every T iterations. This approach is also used in second-order algorithms such as KFAC and Shampoo. We also do not apply the computed learning rates in the first few epochs; rather, we only use them to warm-up the moving average estimates; (see 9 in Appendix .) We incorporate weight-decay with the tuneable hyper-parameter γ by adding the term $\gamma \boldsymbol{W}_k^{(\lambda)}$ to the direction $d_k^{(\lambda)}$ when computing the layer-wise adaptive steps $t_k^{(\lambda)}$.

Full description of algorithms: The pseudocode that fully describes our layer-wise step-size procedure for SGD with momentum (SGD-m-LW) and AdamW (AdamW-LW) is given, respectively, in Algorithm 2 and Algorithm 3 in the Appendix A.1.

6 Experiments

In this section, we compare SGD-m-LW and AdamW-LW with some SOTA **fine-tuned learning rate** first-order (SGD-m, AdamW) and second-order (KFAC, Shampoo) methods. Since SGD-m-LW and AdamW-LW use layer-wise step sizes to scale the directions, fine-tuned SGD-m and AdamW were obvious choices for comparison. We also included KFAC and Shampoo in our tests as SGD-m-LW and AdamW-LW also use information about the local curvature of the loss function. We used the most popular version of Adam, AdamW [29] as a representative of adaptive first-order methods. Our experiments were run on a computer with one V100 GPU and eight Xeon Gold 6248 CPUs using PyTorch [39]. Each algorithm was run using the best hyper-parameters, determined by a grid search (see Appendix B for more details).

CNN problems: We first compared the performance of SGD-m-LW and AdamW-LW to SGD-m, Adam, KFAC and Shampoo on three CNN models, namely, VGG16 [46], ResNet-18 [17], and DenseNet [19], respectively, on the datasets CIFAR-10, CIFAR-100 and SVHN [22]. The first two have 50,000 training data and 10,000 testing data (used as the validation set in our experiments), while SVHN has 73,257 training data and 26,032 testing data. For all algorithms, we used a batch size of 512. In training, we applied data augmentation as described in [23], including random horizontal flip and random crop, since these setting choices have been used and endorsed in many previous research papers, e.g. [54, 7, 42]. (see Appendix B.1 for more details)

All methods (except SGD-m-LW and AdamW-LW) employed a tunable LR schedule that decayed the LR by a factor of 0.1 every K epochs, where K was set to 60 and 40, for the first-order methods, and second-order methods, respectively, on all problems. Moreover, weight decay, which has been shown to improve generalization across different optimizers [29, 54], was employed by all of the algorithms, and a grid search on the weight decay factor and the initial LR (for algorithms that employed a tunable LR), based on the criteria of maximal validation classification accuracy was performed. We set the Fisher matrix update frequency $T_1 = 10$ and inverse update frequency $T_2 = 100$ for second-order methods, as in [42] and the frequency of learning rate computation $T = 20$ for SGD-m-LW and AdamW-LW, with a warm-up period of the first 10 epochs using a fixed warm-up LR of 0.001. In Appendix D, we explore the sensitivity of both AdamW-LW and SGD-m-LW to the choice of T from the set $\mathcal{T} = \{5, 10, 15, 20, 25\}$ on the CIFAR-10 + VGG16 problem. As shown there in Figure 8, the accuracy achieved after 200, epochs by both methods is very insensitive to the chosen value of $T \in \mathcal{T}$ except that SGD-m-LW becomes unstable for $T = 25$. Finally, the damping parameter was set to 1e-8 for Adam (following common practice), and 0.03 for KFAC (`https://github.com/alecwangcq/KFAC-Pytorch`), and for Shampoo, we set $\epsilon = 0.01$.

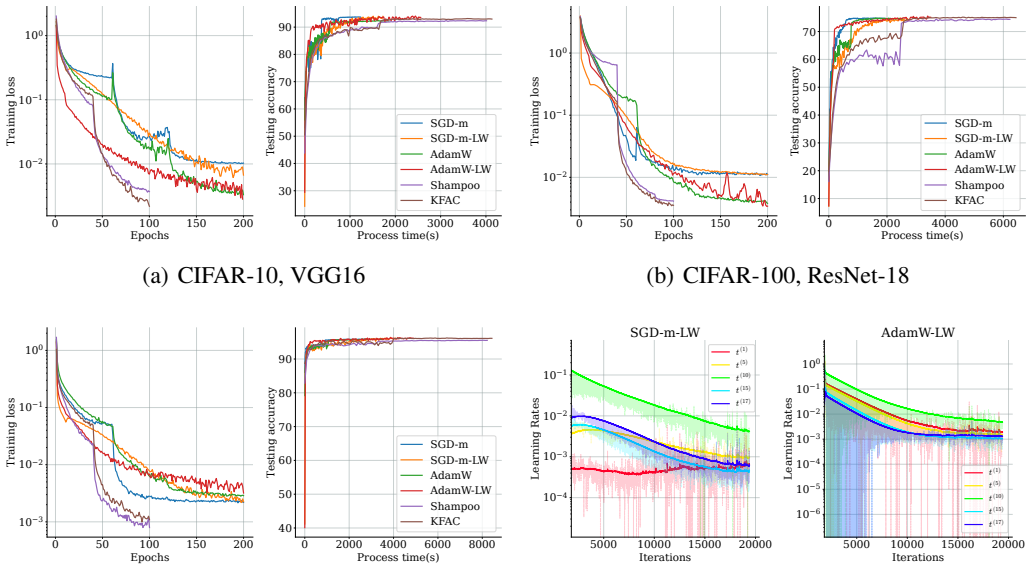

(a) CIFAR-10, VGG16

(b) CIFAR-100, ResNet-18

(c) SVHN, DenseNet

(d) CIFAR-10, VGG16 learning rates

Figure 2: Performance of KFAC, Shampoo, Adam, Adam-LW, SGD-m and SGD-m-LW on three CNN problems (Figures (a), (b) and (c)). Layer-wise learning rate $t^{(\lambda)}$ plots for layers $\lambda = 1, 5, 10, 15, 17$ produced by SGD-LW and Adam-LW on CIFAR-10, VGG16 (Figure (d)).

From Figure 2, we see that SGD-m-LW and AdamW-LW have a similar (and sometimes better) optimization and generalization performance compared to fine-tuned standard versions of SGD-m and AdamW, and do not require any tuning procedure for the learning rate. Moreover, in terms of process time, SGD-m-LW and AdamW-LW are roughly a factor of 1.8 times slower than SGD-m and AdamW and are competitive with all of the SOTA first and second-order methods in our experiments.

Graph Convolutional Networks (GCN) Problems: In this section, we compare the algorithms on a 3-layer GCN for the task of node classification in graphs applied to three citation datasets, Cora, CiteSeer, and PubMed. (see [45] and Appendix B.3 for more details about the experiment setup).

In our experiments, we used a 3-layer GCN with the following node sizes $[I, 128, 64, O]$, where I and O are the numbers of input features and classes, respectively. In the first and second layers of this GCN, the activation function ReLU was followed by a dropout function with a rate of 0.5. The loss function was evaluated as the negative log-likelihood of Softmax of the last layer. The models were trained for 300 epochs. The hyperparameter search space was the same as that used for the CNN problems with no LR schedule and no weight decay, as in this section, we want to focus on the optimization performance of the proposed methods. We set the inverse update frequency $T_2 = 25$ for KFAC and Shampoo and the LR update frequency $T = 1$ for SGD-m-LW and AdamW-LW with no warm-period. We chose $T = 1$ in these problems as each iteration corresponds to a full pass over the dataset, and therefore skipping epochs leads to an unstable optimization procedure as opposed to CNN problems where each epoch has many mini-batch iterations. We use a warm-up period of 10 epochs with $lr0 = 0.001$ as the initial warm-up learning rate value; (see Appendix E for empirical evidence of the insensitivity of the method with respect to choice of $lr0$).

From Figure 3, we see that SGD-m-LW and AdamW-LW were competitive with all of the SOTA first and second-order methods.

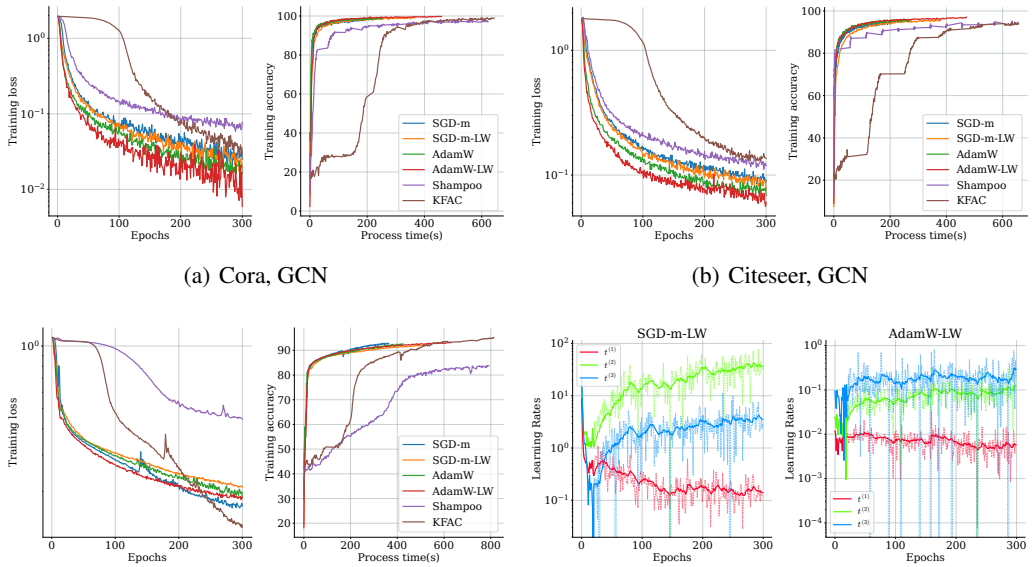

(a) Cora, GCN

(b) Citeseer, GCN

(c) Pubmedm, GCN

(d) Cora, GCN learning rates

Figure 3: Performance of KFAC, Shampoo, Adam, Adam-LW, SGD-m and SGD-m-LW on three GCN problems (Figures (a), (b) and (c)). Layer-wise learning rate $t^{(\lambda)}$ plots for layers $\lambda = 1, 2, 3$ produced by SGD-LW and Adam-LW on Cora, GCN (Figure (d)).

We also report the computed adaptive step sizes per layer in Figures 2-(d) and 3-(d), where the solid curves depict the moving average of the LRs computed every T iteration; while the lighter, highly variable spikes correspond to LRs computed at every iteration. There are two main interesting observations that we identified from these results: the adaptive learning rates have different scales across different layers and the values of the latter are stationary in the sense that one could "learn" a fixed "good" stationary learning rate for each layer without having to recompute it at every iteration.

These results suggest that the layer-wise scaling of the SGD-m and AdamW directions due to using different LRs for each layer, effects the update directions. Therefore, we computed and reported in Figure 4 the cosine similarity between the directions produced by the layer-wise methods and that of their vanilla counterparts in two of the GCN problems; (see next section and section B.4 in Appendix for more details about the cosine computation).

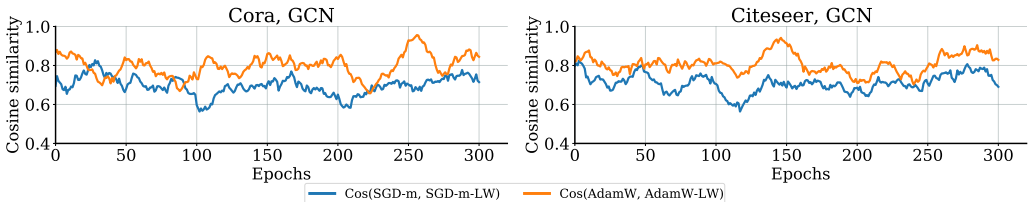

Figure 4: Cosine similarity between the directions produced by the layer-wise methods and that of their vanilla counterparts.

Autoencoder problems: In this section, we compare the optimization performance of the algorithms on two autoencoder problems [18] with datasets MNIST[25], and FACES, which were also used for benchmarking algorithms in [31, 32, 5, 12]. The hyperparameter search space for all SOTA algorithms was the same as the one used in the latter papers. The details of the layer shapes of the Autoencoders are specified in Appendix B.2. Each algorithm was run for 500 seconds for MNIST and 2000 seconds for FACES. We set the Fisher matrix update frequency $T_1 = 1$ and inverse update frequency $T_2 = 20$ for second-order methods, as in [42] and $T = 20$ for SGD-m-LW and AdamW-LW with a 10 epochs warm-up period. From Figure 5, it is clear that SGD-m-LW and AdamW-LW have slightly better optimization performance than their fixed learning rate counterparts, both in terms of per-epoch progress and process time. We postulate that the performance of SGD-m-LW and AdamW-LW is due to the incorporation of curvature information through the layer-wise scaling of the SGD-m and AdamW directions as observed in Figure 4.

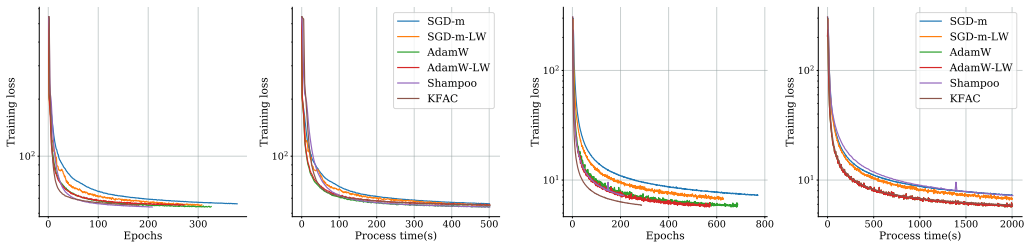

(a) MNIST, Autoencoder

(b) FACES, Autoencoder

Figure 5: Performance of KFAC, Shampoo, Adam, Adam-LW, SGD-m and SGD-m-LW on two Autoencoder problems.

7 Conclusion and Next Steps

We presented a layer-wise step-size procedure for first-order optimization methods that we believe is a valuable tool for fast and practical optimization without learning-rate tuning, especially in DNN applications. Obtaining theoretical convergence guarantees for our method applied to DNNs, whose loss functions are nonconvex functions of the full set of network parameters, and application of our adaptive framework to other variants of SGD and stochastic second-order methods, are interesting topics for future research. In particular, we are interested in adapting and extending the analysis in [13] to our method, and in making use of the underlying multi-affine nature of the loss function in terms of the LW blocks of parameters, when ReLU activation is used. We have explored using the LW LR approach in CNN, GCN and Autoencoder problems, and we are interested in extending our method to other architectures such as RNNs and Transformers and other classes of problems. Finally, considering the use of Hutchinson's method as in [52] to approximate the diagonal of the Hessian to compute the approximate local norms used in our algorithm is an interesting avenue for future work.

8 Limitations

Standard PyTorch's forward and backward functions in autograd are not capable of efficiently computing layer-wise local norms and other layer-wise functions. Providing such capabilities would lead to significant computational and memory-saving improvements for our layerwise approach and others like it.

References

[1] Francis R. Bach. Self-concordant analysis for logistic regression. *ArXiv*, abs/0910.4627, 2009.

[2] Achraf Bahamou, Donald Goldfarb, and Yi Ren. A mini-block fisher method for deep neural networks. In Francisco Ruiz, Jennifer Dy, and Jan-Willem van de Meent, editors, *Proceedings of The 26th International Conference on Artificial Intelligence and Statistics*, volume 206 of *Proceedings of Machine Learning Research*, pages 9191–9220. PMLR, 25–27 Apr 2023.

[3] D.P. Bertsekas, A. Nedić, and A.E. Ozdaglar. *Convex Analysis and Optimization*. Athena Scientific, 2003.

[4] Aleksandar Botev, Hippolyt Ritter, and David Barber. Practical gauss-newton optimisation for deep learning. *ICML 2017*, abs/1706.03662, 2017.

[5] Aleksandar Botev, Hippolyt Ritter, and David Barber. Practical gauss-newton optimisation for deep learning. In *International Conference on Machine Learning*, pages 557–565. PMLR, 2017.

[6] Jie Chen, Tengfei Ma, and Cao Xiao. Fastgcn: fast learning with graph convolutional networks via importance sampling. *arXiv preprint arXiv:1801.10247*, 2018.

[7] Dami Choi, Christopher J Shallue, Zachary Nado, Jaehoon Lee, Chris J Maddison, and George E Dahl. On empirical comparisons of optimizers for deep learning. *arXiv preprint arXiv:1910.05446*, 2019.

[8] John Duchi, Elad Hazan, and Yoram Singer. Adaptive subgradient methods for online learning and stochastic optimization. *J. Mach. Learn. Res.*, 12:2121–2159, July 2011.

[9] Wenbo Gao and Donald Goldfarb. Quasi-newton methods: superlinear convergence without line searches for self-concordant functions. *Optimization Methods and Software*, 34(1):194–217, 2019.

[10] Guillaume Garrigos and Robert M. Gower. Handbook of convergence theorems for (stochastic) gradient methods, 2023.

[11] Behrooz Ghorbani, Shankar Krishnan, and Ying Xiao. An investigation into neural net optimization via hessian eigenvalue density. In Kamalika Chaudhuri and Ruslan Salakhutdinov, editors, *Proceedings of the 36th International Conference on Machine Learning*, volume 97 of *Proceedings of Machine Learning Research*, pages 2232–2241, Long Beach, California, USA, 09–15 Jun 2019. PMLR.

[12] Donald Goldfarb, Yi Ren, and Achraf Bahamou. Practical quasi-newton methods for training deep neural networks. In H. Larochelle, M. Ranzato, R. Hadsell, M. F. Balcan, and H. Lin, editors, *Advances in Neural Information Processing Systems*, volume 33, pages 2386–2396. Curran Associates, Inc., 2020.

[13] Robert Gower, Othmane Sebbouh, and Nicolas Loizou. Sgd for structured nonconvex functions: Learning rates, minibatching and interpolation. In *International Conference on Artificial Intelligence and Statistics*, pages 1315–1323. PMLR, 2021.

[14] Robert M. Gower, Mathieu Blondel, Nidham Gazagnadou, and Fabian Pedregosa. Cutting some slack for sgd with adaptive polyak stepsizes, 2022.

[15] Robert M. Gower, Aaron Defazio, and Michael G. Rabbat. Stochastic polyak stepsize with a moving target. *CoRR*, abs/2106.11851, 2021.

[16] Vineet Gupta, Tomer Koren, and Yoram Singer. Shampoo: Preconditioned stochastic tensor optimization. In Jennifer Dy and Andreas Krause, editors, *Proceedings of the 35th International Conference on Machine Learning*, volume 80 of *Proceedings of Machine Learning Research*, pages 1842–1850. PMLR, 2018.

[17] Kaiming He, Xiangyu Zhang, Shaoqing Ren, and Jian Sun. Deep residual learning for image recognition. In *Proceedings of the IEEE conference on computer vision and pattern recognition*, pages 770–778, 2016.

[18] Geoffrey E Hinton and Ruslan R Salakhutdinov. Reducing the dimensionality of data with neural networks. *science*, 313(5786):504–507, 2006.

[19] Gao Huang, Zhuang Liu, and Kilian Q. Weinberger. Densely connected convolutional networks. *CoRR*, abs/1608.06993, 2016.

[20] Nitish Shirish Keskar and Richard Socher. Improving generalization performance by switching from adam to SGD. *CoRR*, abs/1712.07628, 2017.

[21] Diederik P. Kingma and Jimmy Ba. Adam: A method for stochastic optimization. *CoRR*, abs/1412.6980, 2014.

[22] Alex Krizhevsky, Geoffrey Hinton, et al. Learning multiple layers of features from tiny images. 2009.

[23] Alex Krizhevsky, Ilya Sutskever, and Geoffrey E Hinton. Imagenet classification with deep convolutional neural networks. *Advances in neural information processing systems*, 25:1097–1105, 2012.

[24] Remi Leblond, Fabian Pedregosa, and Simon Lacoste-Julien. Improved asynchronous parallel optimization analysis for stochastic incremental methods. *Journal of Machine Learning Research*, 19(81):1–68, 2018.

[25] Yann LeCun, Corinna Cortes, and CJ Burges. MNIST handwritten digit database. *ATT Labs [Online]. Available: http://yann.lecun.com/exdb/mnist*, 2, 2010.

[26] Shuang Li, William J. Swartworth, Martin Takáč, Deanna Needell, and Robert M. Gower. Sp2: A second order stochastic polyak method, 2022.

[27] Jinxiu Liang, Yong Xu, Chenglong Bao, Yuhui Quan, and Hui Ji. Barzilai–borwein-based adaptive learning rate for deep learning. *Pattern Recognition Letters*, 128:197–203, 2019.

[28] Nicolas Loizou, Sharan Vaswani, Issam Hadj Laradji, and Simon Lacoste-Julien. Stochastic polyak step-size for sgd: An adaptive learning rate for fast convergence. In Arindam Banerjee and Kenji Fukumizu,

editors, *Proceedings of The 24th International Conference on Artificial Intelligence and Statistics*, volume 130 of *Proceedings of Machine Learning Research*, pages 1306–1314. PMLR, 13–15 Apr 2021.

[29] Ilya Loshchilov and Frank Hutter. Decoupled weight decay regularization. In *International Conference on Learning Representations*, 2019.

[30] Maren Mahsereci and Philipp Hennig. Probabilistic line searches for stochastic optimization. *CoRR*, abs/1502.02846, 2015.

[31] James Martens. Deep learning via hessian-free optimization. In *ICML*, volume 27, pages 735–742, 2010.

[32] James Martens and Roger Grosse. Optimizing neural networks with kronecker-factored approximate curvature. In *International conference on machine learning*, pages 2408–2417. PMLR, 2015.

[33] Konstantin Mishchenko and Yura Malitsky. Adaptive gradient descent without descent. In *37th International Conference on Machine Learning (ICLM 2020)*, 2020.

[34] Yu . Nesterov and Arkadi S. Nemirovsky. Interior-point polynomial methods in convex programming. 1994.

[35] Y. E. Nesterov. A method for solving the convex programming problem with convergence rate $o(1/k^2)$. *Dokl. Akad. Nauk SSSR*, 269:543–547, 1983.

[36] Lam M. Nguyen, Phuong Ha Nguyen, Marten van Dijk, Peter Richtárik, Katya Scheinberg, and Martin Takáč. Sgd and hogwild! convergence without the bounded gradients assumption. *ICML 2018*, 2018.

[37] Antonio Orvieto, Simon Lacoste-Julien, and Nicolas Loizou. Dynamics of sgd with stochastic polyak stepsizes: Truly adaptive variants and convergence to exact solution, 2022.

[38] Courtney Paquette and Katya Scheinberg. A stochastic line search method with expected complexity analysis. *SIAM Journal on Optimization*, 30(1):349–376, 2020.

[39] Adam Paszke, Sam Gross, Francisco Massa, Adam Lerer, James Bradbury, Gregory Chanan, Trevor Killeen, Zeming Lin, Natalia Gimelshein, Luca Antiga, Alban Desmaison, Andreas Kopf, Edward Yang, Zachary DeVito, Martin Raison, Alykhan Tejani, Sasank Chilamkurthy, Benoit Steiner, Lu Fang, Junjie Bai, and Soumith Chintala. Pytorch: An imperative style, high-performance deep learning library. In H. Wallach, H. Larochelle, A. Beygelzimer, F. d'Alché-Buc, E. Fox, and R. Garnett, editors, *Advances in Neural Information Processing Systems 32*, pages 8024–8035. Curran Associates, Inc., 2019.

[40] Barak A. Pearlmutter. Fast exact multiplication by the hessian. *Neural Comput.*, 6(1):147–160, Jan. 1994.

[41] Boris Polyak. Some methods of speeding up the convergence of iteration methods. *Ussr Computational Mathematics and Mathematical Physics*, 4:1–17, 12 1964.

[42] Yi Ren and Donald Goldfarb. Tensor normal training for deep learning models. In A. Beygelzimer, Y. Dauphin, P. Liang, and J. Wortman Vaughan, editors, *Advances in Neural Information Processing Systems*, 2021.

[43] Herbert Robbins and Sutton Monro. A stochastic approximation method. *The Annals of Mathematical Statistics*, 22(3):400–407, 1951.

[44] Fabian Schaipp, Robert M. Gower, and Michael Ulbrich. A stochastic proximal polyak step size, 2023.

[45] Prithviraj Sen, Galileo Namata, Mustafa Bilgic, Lise Getoor, Brian Galligher, and Tina Eliassi-Rad. Collective classification in network data. *AI magazine*, 29(3):93–93, 2008.

[46] Karen Simonyan and Andrew Zisserman. Very deep convolutional networks for large-scale image recognition. *arXiv preprint arXiv:1409.1556*, 2014.

[47] Tianxiao Sun and Quoc Tran-Dinh. Generalized self-concordant functions: a recipe for newton-type methods. *Mathematical Programming*, 178(1-2):145–213, 2019.

[48] Conghui Tan, Shiqian Ma, Yu-Hong Dai, and Yuqiu Qian. Barzilai-borwein step size for stochastic gradient descent. *Advances in neural information processing systems*, 29, 2016.

[49] T. Tieleman and G. Hinton. Lecture 6.5—RmsProp: Divide the gradient by a running average of its recent magnitude. COURSERA: Neural Networks for Machine Learning, 2012.

[50] Quoc Tran-Dinh, Yen-Huan Li, and Volkan Cevher. Composite convex minimization involving self-concordant-like cost functions. In *MCO*, 2015.

[51] Sharan Vaswani, Aaron Mishkin, Issam H. Laradji, Mark Schmidt, Gauthier Gidel, and Simon Lacoste-Julien. Painless stochastic gradient: Interpolation, line-search, and convergence rates. *CoRR*, abs/1905.09997, 2019.

[52] Zhewei Yao, Amir Gholami, Sheng Shen, Kurt Keutzer, and Michael W Mahoney. Adahessian: An adaptive second order optimizer for machine learning. *AAAI (Accepted)*, 2021.

[53] Matthew D. Zeiler. ADADELTA: An Adaptive Learning Rate Method. *CoRR*, abs/1212.5701, 2012.

[54] Guodong Zhang, Chaoqi Wang, Bowen Xu, and Roger Grosse. Three mechanisms of weight decay regularization. In *International Conference on Learning Representations*, 2019.

[55] Yuchen Zhang and Xiao Lin. Disco: Distributed optimization for self-concordant empirical loss. In Francis Bach and David Blei, editors, *Proceedings of the 32nd International Conference on Machine Learning*, volume 37 of *Proceedings of Machine Learning Research*, pages 362–370, Lille, France, 07–09 Jul 2015. PMLR.

[56] Chaoxu Zhou, Wenbo Gao, and Donald Goldfarb. Stochastic adaptive quasi-Newton methods for minimizing expected values. In Doina Precup and Yee Whye Teh, editors, *Proceedings of the 34th International*

Conference on Machine Learning, volume 70 of *Proceedings of Machine Learning Research*, pages 4150–4159. PMLR, 06–11 Aug 2017.

A Appendix

A.1 Full algorithm descriptions

Algorithm 2: SGD-m-LW: Per-Layer Adaptive Step-Size for SGD-m

Input: Initial iterate $\boldsymbol{W}_0$, batch size m, and max number of iterations N.
Betas $\beta, \beta_t = 0.9, 0.99$, Weight-decay γ, Update-frequency T.
Initialize $m_k \leftarrow 0$, $t_k^{(\lambda)} \leftarrow 0$
for $k = 1 \cdots N$ **do**
  Sample m samples S_k.
  Compute $g_k = \nabla F_{S_k}(\boldsymbol{W}_k)$.
  Compute $m_k = \beta m_{k-1} + g_k$
  for $l = 1 \dots L$ **do**
    Compute $d_k^{(\lambda)} = m_k^{(\lambda)} + \gamma \boldsymbol{W}_k^{(\lambda)}$
    if $k \mod T = 0$ **then**
      Compute $\rho^{(\lambda)} = {d_k^{(\lambda)}}^\top g_k^{(\lambda)}$.
      Compute $\delta^{(\lambda)} = \sqrt{{d_k^{(\lambda)}}^\top H_k^{(\lambda)} d_k^{(\lambda)}}$.
      $t_k^{(\lambda)} \leftarrow \beta_t t_{k-1}^{(\lambda)} + (1-\beta_t)\frac{1}{L}\frac{\rho^{(\lambda)}}{\left(\rho^{(\lambda)}+\delta^{(\lambda)}\right)\delta^{(\lambda)}}$
    $W_{k+1}^{(\lambda)} \leftarrow W_k^{(\lambda)} - t_k^{(\lambda)} d_k^{(\lambda)}$

Algorithm 3: AdamW-LW: Per-Layer Adaptive Step-Size for AdamW

Input: Initial iterate $\boldsymbol{W}_0$, batch size m, and max number of iterations N.
Betas $\beta_1, \beta_2, \beta_t = 0.9, 0.999, 0.99$, Damping $\epsilon = 10^{-8}$, Weight-decay γ, Update-frequency T.
Initialize $m_k \leftarrow 0$, $v_k \leftarrow 0$, $t_k^{(\lambda)} \leftarrow 0$
for $k = 1 \cdots N$ **do**
  Sample m samples S_k.
  Compute $g_k = \nabla F_{S_k}(\boldsymbol{W}_k)$.
  Compute $m_k = \beta_1 m_{k-1} + (1-\beta_1) g_k, \quad v_k = \beta_2 v_{k-1} + (1-\beta_2) g_k^2$
  Compute $\hat{m}_k = \frac{m_k}{(1-\beta_1^k)}, \quad \hat{v}_k = \frac{v_k}{(1-\beta_2^k)}$
  for $l = 1 \dots L$ **do**
    Compute $d_k^{(\lambda)} = \frac{\hat{m}_k^{(\lambda)}}{\sqrt{\hat{v}_k^{(\lambda)}+\epsilon}} + \gamma \boldsymbol{W}_k^{(\lambda)}$
    if $k \mod T = 0$ **then**
      Compute $\rho^{(\lambda)} = {d_k^{(\lambda)}}^\top g_k^{(\lambda)}$.
      Compute $\delta^{(\lambda)} = \sqrt{{d_k^{(\lambda)}}^\top H_k^{(\lambda)} d_k^{(\lambda)}}$.
      $t_k^{(\lambda)} \leftarrow \beta_t t_{k-1}^{(\lambda)} + (1-\beta_t)\frac{1}{L}\frac{\rho^{(\lambda)}}{\left(\rho^{(\lambda)}+\delta^{(\lambda)}\right)\delta^{(\lambda)}}$
    $W_{k+1}^{(\lambda)} \leftarrow W_k^{(\lambda)} - t_k^{(\lambda)} d_k^{(\lambda)}$

A.2 Proof of Theorem 1

Proof of Theorem 1. The proof is a consequence of Lemma 1 (Lemma 4.1 in [9]), judiciously applied to the layer-wise restricted functions $F^{(\lambda)}(\cdot)$. More specifically, since we are considering the direction given by SGD-LW, we have $d_k^{(\lambda)} = g_k^{(\lambda)}$ and the overall direction of the SGD-LW is given by concatenating the vectors $t_k^{(\lambda)} d_k^{(\lambda)}$, for $\lambda = 1 \dots L$, into an overall step $\hat{p}$ which can be expressed

as the convex combination $\hat{p} = \sum_{\lambda=0}^{L} \frac{1}{L}\hat{p}^{(\lambda)}$ of the vectors

$$\hat{p}^{(\lambda)} = \left[\mathbf{0}^{(1)}, ..., \frac{\rho^{(\lambda)}}{\left(\rho^{(\lambda)} + \delta^{(\lambda)}\right)\delta^{(\lambda)}} d_k^{(\lambda)}, ..., \mathbf{0}^{(L)}\right], \quad \text{for } \lambda = 1, \ldots, L.$$

Therefore,

$$\begin{aligned} F(\boldsymbol{W}_k - \hat{p}) &= F\left(\frac{1}{L}\sum_{\lambda=0}^{L}\left(\boldsymbol{W}_k - \hat{p}^{(\lambda)}\right)\right) \\ &\overset{(a)}{\leq} \frac{1}{L}\sum_{\lambda=0}^{L} F\left(\boldsymbol{W}_k - \hat{p}^{(\lambda)}\right) \overset{(b)}{=} \frac{1}{L}\sum_{\lambda=0}^{L} F^{(\lambda)}\left(\boldsymbol{W}_k^{(\lambda)} - \frac{\rho^{(\lambda)}}{\left(\rho^{(\lambda)} + \delta^{(\lambda)}\right)\delta^{(\lambda)}} d_k^{(\lambda)}\right) \\ &\overset{(c)}{\leq} \frac{1}{L}\sum_{\lambda=0}^{L} F^{(\lambda)}\left(\boldsymbol{W}_k^{(\lambda)}\right) - \Delta(\delta^{(\lambda)}, \frac{\rho^{(\lambda)}}{\left(\rho^{(\lambda)} + \delta^{(\lambda)}\right)\delta^{(\lambda)}}), \end{aligned}$$

where $\Delta(\delta_k, t) = (\delta_k + \rho_k)t + log(1 - \delta_k t)$. In (a), we used the convexity of F by Assumption A1, in (b), we used the definition of the vectors $\hat{p}^{(\lambda)}$ and the restricted loss functions $F^{(\lambda)}(\cdot)$, and in (c), we applied Lemma 1 to the latter functions. We have:

$$\Delta(\delta^{(\lambda)}, \frac{\rho^{(\lambda)}}{\left(\rho^{(\lambda)} + \delta^{(\lambda)}\right)\delta^{(\lambda)}}) = \omega\left(\eta_k^{(\lambda)}\right), \quad \text{where } \omega(z) = z - \log(1+z) \text{ and } \eta_k^{(\lambda)} = \frac{\rho_k^{(\lambda)}}{\delta_k^{(\lambda)}}.$$

Hence, we have:

$$F(\boldsymbol{W}_k - \hat{p}) \overset{(d)}{\leq} F(\boldsymbol{W}_k) - \frac{1}{L}\sum_{\lambda=0}^{L}\omega\left(\eta_k^{(\lambda)}\right),$$

where in (d), we used the fact that $F^{(\lambda)}\left(\boldsymbol{W}_k^{(\lambda)}\right) = F(\boldsymbol{W}_k)$. Furthermore, we have:

$$\eta_k^{(\lambda)} = \frac{\rho_k^{(\lambda)}}{\delta_k^{(\lambda)}} = \frac{\|g_k^{(\lambda)}\|^2}{\sqrt{{g_k^{(\lambda)}}^\top H_k^{(\lambda)} g_k^{(\lambda)}}} \leq \frac{\|g_k^{(\lambda)}\|}{m} \leq \frac{\gamma}{m},$$

where we used Assumptions A1 and A2 in the last two inequalities, respectively. By observing that $\omega(z) = z - log(1+z)$ satisfies $\omega(z) \geq \frac{1}{2}(1+\Gamma)^{-1}z^2$ for all $z \in [0, \Gamma]$, we have:

$$F(\boldsymbol{W}_k - \hat{p}) \leq F(\boldsymbol{W}_k) - \frac{1}{2L(1+\frac{\gamma}{\sqrt{m}})}\sum_{\lambda=0}^{L}(\eta_k^{(\lambda)})^2.$$

Using Assumption A1, we obtain the following lower bound on the term $\sum_{\lambda=0}^{L}(\eta_k^{(\lambda)})^2$:

$$\begin{aligned} \sum_{\lambda=0}^{L}(\eta_k^{(\lambda)})^2 &= \sum_{\lambda=0}^{L}\frac{\|g_k^{(\lambda)}\|^4}{{g_k^{(\lambda)}}^\top H_k^{(\lambda)} g_k^{(\lambda)}} \geq \sum_{\lambda=0}^{L}\frac{\|g_k^{(\lambda)}\|^4}{M\|g_k^{(\lambda)}\|^2} \\ &\geq \frac{1}{M}\sum_{\lambda=0}^{L}\|g_k^{(\lambda)}\|^2 := \frac{1}{M}\|\nabla F(\boldsymbol{W}_k)\|^2. \end{aligned}$$

Therefore, we obtain

$$F(\boldsymbol{W}_k - \hat{p}) = F(\boldsymbol{W}_{k+1}) \leq F(\boldsymbol{W}_k) - \frac{1}{2ML(1+\frac{\gamma}{\sqrt{m}})}\|\nabla F(\boldsymbol{W}_k)\|^2. \tag{6}$$

It is well known [3] that for strongly convex functions:

$$\|\nabla F(\boldsymbol{W}_k)\|^2 \geq 2m[F(\boldsymbol{W}_k) - F(\boldsymbol{W}^*)].$$

Using this inequality to upper-bound $-\|\nabla F(\boldsymbol{W}_k)\|^2$ in (6) and subtracting $F(\boldsymbol{W}^*)$ from both sides, we obtain:

$$F(\boldsymbol{W}_{k+1}) - F(\boldsymbol{W}^*) \leq \rho(F(\boldsymbol{W}_k) - F(\boldsymbol{W}^*)),$$

with

$$\rho = 1 - \frac{m}{ML(1+\frac{\gamma}{\sqrt{m}})}.$$

The theorem then follows by induction on k.

□

B Experiment Details

B.1 Experiment Settings for the CNN Problems

The ResNet18 model refers to the one in Table 6 of [17], the VGG16 model refers to model D of [46] with the modification that batch normalization layers were added after all of the convolutional layers in the model, and the DenseNet model refers to the DenseNet-121 model in [19]. For all algorithms, we used a batch size of 512 at every iteration.

We used weight decay for all the algorithms that we tested, which is related to, but not the same as L_2 regularization added to the loss function, and has been shown to help improve generalization performance across different optimizers [29, 54]. For KFAC, we set the overall damping value to be 0.03, as suggested in the implementation in `https://github.com/alecwangcq/KFAC-Pytorch`.

In order to obtain Figure 2, we first conducted a grid search on the initial learning rate (lr) and weight decay (wd) factor based on the criteria of maximizing the classification accuracy on the validation set. Table 1 gives, for each of the algorithms in our tests, the hyper-parameter lr and wd values that were included in our grid search.

Table 1: Grid of hyper-parameters for CNN problems

Algorithm	learning rate	weight decay γ
SGD-m	3e-5, 1e-4, 3e-4, 1e-3, 3e-3, 1e-2, 3e-2, 1e-1, 3e-1, 1e0	1e-2, 3e-2, 1e-1, 3e-1, 1e0, 3e0, 1e1
SGD-m-LW	–	1e-2, 3e-2, 1e-1, 3e-1, 1e0, 3e0, 1e1
AdamW	1e-6, 3e-6, 1e-5, 3e-5, 1e-4, 3e-4, 1e-3, 3e-3, 1e-2, 3e-2	1e-2, 3e-2, 1e-1, 3e-1, 1e0, 3e0, 1e1
AdamW-LW	–	1e-2, 3e-2, 1e-1, 3e-1, 1e0, 3e0, 1e1
Shampoo	3e-5, 1e-4, 3e-4, 1e-3, 3e-3, 1e-2, 3e-2, 1e-1 3e-1	1e-2, 3e-2, 1e-1, 3e-1, 1e0, 3e0, 1e1
KFAC	3e-6, 1e-5, 3e-5, 1e-4, 3e-4, 1e-3, 3e-3, 1e-2, 3e-2	1e-2, 3e-2, 1e-1, 3e-1, 1e0, 3e0, 1e1

The best hyper-parameter values that were determined in our grid search and the testing accuracy achieved using those values are listed in Table 2. In addition, for each problem we highlight in clarify: choose a color the best testing accuracy achieved.

Table 2: Hyper-parameters (initial learning rate, weight decay factor) used to produce Figure 2, and the testing accuracy achieved

Name	CIFAR-10 + VGG16	CIFAR-100 + ResNet-18	SVHN + DenseNet121
KFAC	(3e-4, 3e-1) $\rightarrow$ 93.12%	(3e-3, 3e-2) $\rightarrow$ 74.99%	(3e-3, 3e-2) $\rightarrow$ 96.11%
Shampoo	(1e-2, 1e-1) $\rightarrow$ 92.88%	(1e-3, 3e-1) $\rightarrow$ 74.39%	(3e-3, 1e-1) $\rightarrow$ 95.51%
AdamW-LW	(-, 1e-1) $\rightarrow$ 93.58%	(-, 3e0) $\rightarrow$ 75.11%	(-, 3e0) $\rightarrow$ 96.17%
AdamW	(3e-4, 1e0) $\rightarrow$ 92.26%	(1e-3, 3e0) $\rightarrow$ 74.71%	(3e-4, 3e0) $\rightarrow$ 95.81%
SGD-m-LW	(-, 1e-1) $\rightarrow$ 93.94%	(-, 3e-2) $\rightarrow$ 74.62%	(-, 1e-1) $\rightarrow$ 96.01%
SGD-m	(3e-2, 3e-2) $\rightarrow$ 93.66%	(3e-2, 3e-2) $\rightarrow$ 74.69%	(1e-2, 1e-1) $\rightarrow$ 95.85%

B.2 Experiment Settings for the Autoencoder Problems

Table 3 describes the model architectures of the autoencoder problems. The activation functions of the hidden layers are always ReLU, except that there is no activation for the very middle layer.

Table 3: DNN architectures for the MLP autoencoder problems

	Layer width
MNIST	[784, 1000, 500, 250, 30, 250, 500, 1000, 784]
FACES	[625, 2000, 1000, 500, 30, 500, 1000, 2000, 625]

MNIST[1] and FACES[2] contain 60,000 and 103,500 training samples, respectively, which we used in our experiment to train the models and compute the training losses.

We used binary entropy loss (with sigmoid) for MNIST, and squared error loss for FACES. The above settings largely mimic the settings in [31, 32, 5, 42]. Since we primarily focused on optimization rather than generalization in these tasks, we did not include L_2 regularization or weight decay.

In order to obtain Figure 5, we first conducted a grid search on the learning rate (lr) and damping value clarify: should this be ϵ and not λ based on the criteria of minimizing the training loss. The values of these hyper-parameters that were included in our grid searches for each of the algorithms in our tests are specified in Table 4.

Table 4: Grid of hyper-parameters for autoencoder problems

Algorithm	learning rate	damping λ
SGD-m	1e-4, 3e-4, 1e-3, 3e-3, 1e-2, 3e-2	damping: not applicable
SGD-m-LW	-	damping: not applicable
AdamW	1e-5, 3e-5, 1e-4, 3e-4, 1e-3, 3e-3, 1e-2	1e-8, 1e-4, 1e-2
AdamW-LW	-	1e-8, 1e-4, 1e-2
Shampoo	1e-5, 3e-5, 1e-4, 3e-4, 1e-3, 3e-3	1e-4, 3e-4, 1e-3, 3e-3, 1e-2
KFAC	1e-4, 3e-4, 1e-3, 3e-3, 1e-2, 3e-2, 1e-2, 3e-2	1e-2, 3e-2, 1e-1, 3e-1, 1e0, 3e0, 1e1

The best hyper-parameter values determined by our grid searches, and the training loss achieved by those values are listed in Table 5.

Table 5: Hyper-parameters (learning rate, damping) used to produce Figure 5 and the training loss achieved

Name	MNIST	FACES
KFAC	(3e-3, 3e-1) $\rightarrow$ 53.56	(1e-1, 1e1) $\rightarrow$ 5.55
Shampoo	(3e-4, 3e-4) $\rightarrow$ 53.80	(3e-4, 3e-4) $\rightarrow$ 7.21
AdamW-LW	(-, 1e-4) $\rightarrow$ 54.31	(-, 1e-4) $\rightarrow$ 5.61
AdamW	(3e-4, 1e-4) $\rightarrow$ 53.67	(1e-4, 1e-4) $\rightarrow$ 5.55
SGD-m-LW	(-, -) $\rightarrow$ 54.48	(-, -) $\rightarrow$ 6.47
SGD-m	(3e-3, -) $\rightarrow$ 55.63	(1e-3, -) $\rightarrow$ 7.08

B.3 Experiment Settings for the GCN Problems

In this set of experiments, we studied the task of node classification in graphs applied to three citation datasets, Cora, CiteSeer, and PubMed(see [45]). In Table 6, nodes and edges correspond to documents and citation links, respectively, for these datasets. A sparse feature vector of document keywords and a class label are associated with each node. For our experiments, as in [6], for each dataset, we used all of the nodes for training, except for 1000 nodes that were reserved for testing.

Table 6: Citation network datasets statistics

Dataset	Nodes	Edges	Classes	Features
Citeseer	3,327	4732	6	3,703
Cora	2,708	5,429	7	1,433
Pubmed	19,717	44,338	3	500

The hyper-parameter search space was the same as that used for the CNN problems with no LR schedule(see Appendix B.1 for the search space).

[1] `http://yann.lecun.com/exdb/mnist/`

[2] `http://www.cs.toronto.edu/~jmartens/newfaces_rot_single.mat`

B.4 Details regarding the Cosine similarity experiment

As mentioned in the main manuscript, we explored how the layer-wise scaling of the SGD-m and AdamW directions, using different LRs for each layer, effects the update directions. We provide here a detailed implementation of the procedure that we used for completeness. More specifically, for any algorithm X, we reported the cosine similarity between the direction given by X and that obtained by its layer-wise version using the procedure described in Algorithm 4.

Algorithm 4: Cosine(X-LW, X) for Algorithm X

Input: Initial $\boldsymbol{W}_0$, batch size m, number of iterations N and Algorithm X hyper-parameters.

for $k = 1 \cdots N$ **do**

Sample m samples S_k.

Compute $g_k = \nabla F_{S_k}(\boldsymbol{W}_k)$.

Compute d_k Algorithm X direction.

for $\lambda = 1 \dots L$ **do**

Compute $\rho^{(\lambda)} = {d_k^{(\lambda)}}^\top g_k^{(\lambda)}$, $\delta^{(\lambda)} = \sqrt{{d_k^{(\lambda)}}^\top H_k^{(\lambda)} d_k^{(\lambda)}}$

Compute $t_k^{(\lambda)} = \frac{1}{L} \frac{\rho^{(\lambda)}}{\left(\rho^{(\lambda)} + \delta^{(\lambda)}\right)\delta^{(\lambda)}}$

$W_{k+1}^{(\lambda)} \leftarrow W_k^{(\lambda)} - t_k^{(\lambda)} d_k^{(\lambda)}$

Compute and store the cosine $\dfrac{\sum_{\lambda=1}^{L} t_k^{(\lambda)} \left\| d_k^{(\lambda)} \right\|^2}{\sqrt{\sum_{\lambda=1}^{L} {t_k^{(\lambda)}}^2 \left\| d_k^{(\lambda)} \right\|^2} \sqrt{\sum_{\lambda=1}^{L} \left\| d_k^{(\lambda)} \right\|^2}}$

C Comparison against SGD-m and AdamW with various constant learning rates and learning-rate schedules

In this section, we compare how our layer-wise adaptive LR methods perform against the vanilla version of SGD-m and AdamW with various learning rate (lr) values and LR schedules with various initial LR values. In Figure 6, we plot the performance of SGD-m-LW and AdamW-LW against different constant learning rate runs of SGD-m and AdamW, respectively, on the Cora GCN problem.

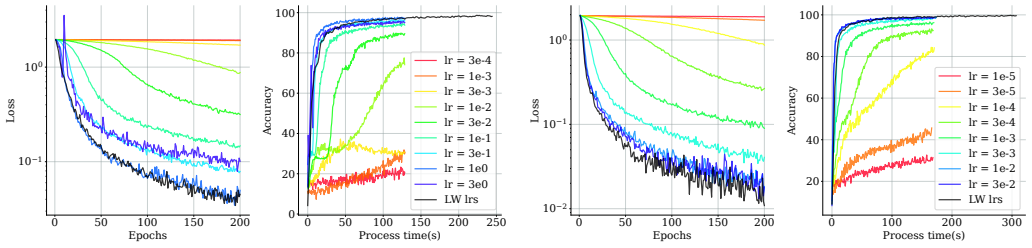

(a) Cora, GCN, SGD-m

(b) Cora, GCN, AdamW

Figure 6: Performance of SGD-m-LW and AdamW-LW in comparison with SGD-m and AdamW with different constant learning rates (lr) on the Cora GCN problem.

In Figure 7, we compare the performance of SGD-m-LW and AdamW-LW against different runs of SGD-m and AdamW, respectively, associated with LR schedules with different initial values on the CIFAR-10 + VGG16 Problem. As in the tests on the CNN problems reported in Section 6, we used a LR schedule that decayed the LR by a factor of 0.1 every 60 epochs.

As can be seen in both Figures 6 and 7, our adaptive layer-wise versions of both SGD-m and AdamW outperform their standard non-layer-wise versions over a wide range of fixed LRs and LR schedules with a wide range of different initial LRs.

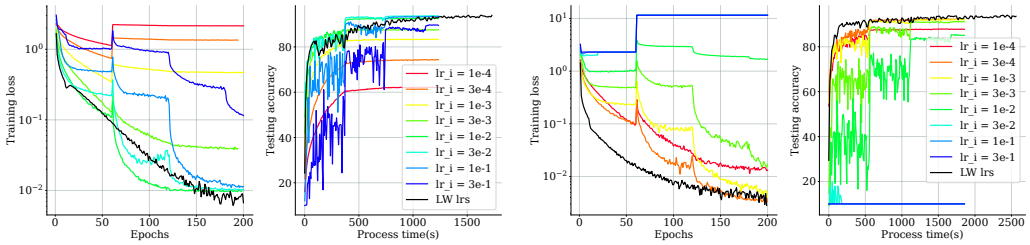

(a) CIFAR-10, VGG16, SGD-m (b) CIFAR-10, VGG16, AdamW

Figure 7: Performance of SGD-m-LW and AdamW-LW in comparison with SGD-m and AdamW using LR schedule with different initial values (lr_i) on CIFAR-10 + VGG16 problem.

D Sensitivity to the learning rate update frequency T

In this section, we investigate the sensitivity of our method to the learning rate update frequency T used to amortize the computational cost over the optimization process. In Figure 8, we illustrate the performance of SGD-m-LW and AdamW-LW varies as a function of the value of T chosen from the set $\mathcal{T} = \{5, 10, 15, 20, 25\}$ on the CIFAR-10 + VGG16 problem. As can be seen there, the accuracy achieved by AdamW-LW, $\text{Acc}_{\mathcal{T}} = \{93.63\%, 93.56\%, 93.49\%, 93.58\%, 93.56\%\}$ and SGD-m-LW, $\text{Acc}_{\mathcal{T}} = \{93.63\%, 93.68\%, 93.69\%, 93.66\%, 13.87\%\}$ is very insensitive to the value of T chosen for the set $\mathcal{T}$, except that SGD-m-LW becomes unstable for $T = 25$. The choice of T has a small effect on the value of the loss function achieved by SGD-m-LW at the end of 200 epochs, and practically no effect for AdamW-LW. However, clearly, the choice of T has a substantial effect on the process time.

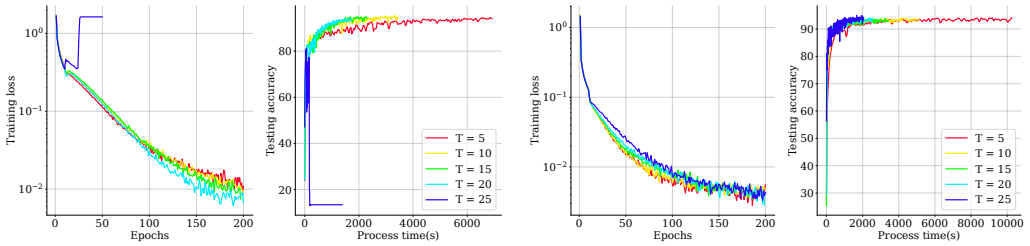

(a) CIFAR-10, VGG16, SGD-m-LW (b) CIFAR-10, VGG16, AdamW-LW

Figure 8: Performance of SGD-m-LW and AdamW-LW with different LR update frequency values T on the CIFAR-10 + VGG16 problem.

E Sensitivity to the warm-up learning rate

In this section, we investigate the sensitivity of our method to the initial learning rate employed during the first few epochs of the optimization process. In Figure 9, we depict the performance of AdamW-LW with 8 different initial warm-up learning rates on the Cora and Citeseer GCN problems.

As shown there, the choice of the warm-up LR had a very small effect on the testing accuracy, and only a small effect on the ultimate training loss achieved.

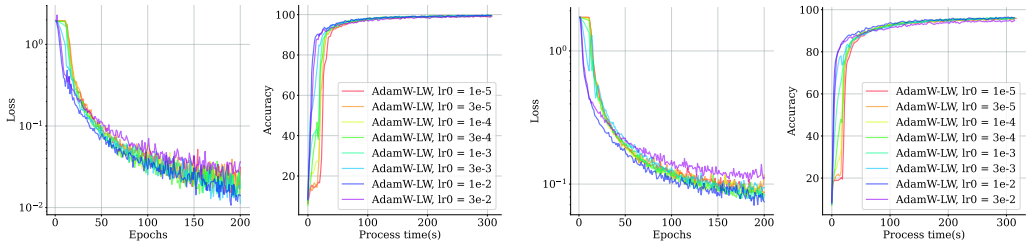

(a) Cora, GCN (b) Citeseer, GCN

Figure 9: Performance of Adam-LW with different initial warm-up learning rates (lr0) on the Cora and Citeseer GCN problems.